

Preformed Excitons, Orbital Selectivity, and Charge-Density-Wave Order in 1T-TiSe₂

S. Koley¹, M. S. Laad³, N. S. Vidhyadhiraja⁴ and A. Taraphder^{1,2}

¹Department of Physics and Centre for Theoretical Studies,
Indian Institute of Technology, Kharagpur 721302 India

² School of Basic Sciences, Indian Institute of Technology, Mandi 175001 India

³Institut Laue Langevin, 6, Rue Jules Horowitz, 38042 Grenoble Cedex, France.

⁴ Jawaharlal Nehru Centre for Advanced Scientific Research, Bangalore 560064 India

Abstract. Traditional routes to Charge-Density-Wave in transition metal dichalcogenides, relying on Fermi surface nesting or Jahn-Teller instabilities have recently been brought into question. While this calls for exploration of alternative views, paucity of theoretical guidance sustains lively controversy on the origin of, and interplay between CDW and superconductive orders in transition metal dichalcogenides. Here, we explore a preformed excitonic liquid route, heavily supplemented by modern correlated electronic structure calculations, to an excitonic-CDW order in 1T-TiSe₂. We show that orbital-selective dynamical localisation arising from preformed excitonic liquid correlations is somewhat reminiscent to states proposed for *d*- and *f*-band quantum criticality at the border of magnetism. Excellent quantitative explication of a wide range of spectral and transport responses in both normal and CDW phases provides strong support for our scenario, and suggests that soft excitonic liquid fluctuations mediate superconductivity in a broad class of transition metal dichalcogenides on the border of CDW. This brings the transition metal dichalcogenides closer to the bad actors in *d*- and *f*-band systems, where anomalously soft fluctuations of electronic origin are believed to mediate unconventional superconductivity on the border of magnetism.

PACS numbers: 71.45.Lr, 71.30.+h, 75.50.Cc

1. Introduction

Twenty six years after the path-breaking discovery of high- T_c superconductivity in doped, quasi-two dimensional copper oxides (cuprates), the list of ill-understood strongly correlated electronic systems (SCES) with partially filled d or f bands continues to grow [1, 2, 3]. The paradigm shift engendered by cuprates also fuelled renewed interest and study of older systems. Before the cuprate revolution, these were sore spots in the standard model of electrons in metals, centred around the celebrated Landau Fermi liquid (LFL) theory. Intense activity to unravel increasing variety of unconventional ordered states with ill-understood metallicity has stabilised this paradigm shift. Cuprates are not, it is now clear, an isolated example: rare-earth systems close to magnetic instabilities at $T = 0$, increasing number of d -band perovskites and the recent explosion in Fe-arsenides are but a few examples of a truly diverse zoo of strange systems.

Perhaps equally remarkable is the fact that careful work in the recent past has brought out unexpected similarities between the newer and older bad actors above. This is best exemplified by the recent revival of interest in quasi-2D transition metal dichalcogenides (TMD). For more than forty years, the origin of charge density wave (CDW) and superconductive (SC) orders and their interplay in the layered TMD had remained ill-understood issues [4, 5]. Historically, appealing to one-electron (density-functional theory) band structure led to the conventional wisdom of CDW arising from Fermi surface (FS) nesting, or via a band Jahn-Teller (JT) instability. Recent revival in the field was stimulated, among other things, by falsification of these views by recent ARPES work [6]. The exciting possibility of an alternative, intrinsically strong coupling view, involving CDW order emerging as a Bose-Einstein condensation (BEC) of an incoherent preformed excitonic liquid (PEL) normal state, arose [7, 8, 9] as an attempt to address this new conflict, and has the potential to bring TMD into the list of strange actors. Indeed, parallels between TMD and cuprates have increasingly been claimed in certain studies [10]. It is also suggested that the absence of magnetism in TMD allows studies of a bad metal without attendant magnetic fluctuations that complicate the physics in cuprates [11]. That a strong coupling scenario for TMD closer to the Mott limit is in order, is shown by the fact that the related system 1T-TaS₂ has long been understood as a Mott insulator [12]: it is then fully conceivable that Mottness also plays important roles in other TMD. From this viewpoint, much as in the more recent examples of intense interest, melting of the excitonic-CDW order in a PEL scenario would necessarily enhance excitonic fluctuations, which could act as an unconventional electronic ‘pairing glue’ for emergence of the competing SC order. However, the theoretical situation still remains unclear, and FS-nesting as well as strong electron-phonon views are still claimed to be the instigators of CDW order and SC in pressurised or doped systems[10].

The long-studied 1T-TiSe₂ is a particularly relevant case in point. Careful experimental work has unravelled behavior that consistently fails to fit into any

conventional views. We list the problems here:

- (i) While optical studies [13] show that the normal-CDW transition is a semi-metal to semiconductor transition a la the Overhauser scenario, noticeable spectral weight transfer (SWT) over an energy scale of order 1.0 eV upon heating from 10K to 300K, along with a clear isosbestic point as a function of temperature (T) below $T_{cdw} = 200$ K and a large normal state scattering rate support sizable electronic correlations.
- (ii) Pure 1T-TiSe₂ shows bad-metallic resistivity, much above the Mott limit, even at pretty low T ($\ll T_{cdw}$), with a maximum, but no anomaly, in $d\rho/dT$ at $T \simeq T_{cdw}$ [14]. Tellingly, recovery of good metallicity at high pressures also destroys SC. Such a correlation is repeatedly seen in many systems where unconventional SC appears near Mott insulators and magnetism [15] (however, TMD never show magnetism, nor has Mottness been hitherto considered important, except for 1T-TaS₂ [12] and 2H-TaSe₂[7, 11]). Thus, whatever causes strong normal state scattering also facilitates SC pair formation below T_c .
- (iii) ARPES data [16] shows that the renormalised electronic structure in the normal state ($T > T_{cdw}$) already resembles an LDA dispersion modified by excitonic correlations, supporting a PEL view. Moreover, lack of clear polaron effects (e.g, kinks in the band dispersion at phonon energies, well below E_F in resonant inelastic X-ray scattering [8]) and, more importantly, the insensitivity of ARPES band dispersions to atomic displacements occurring across T_{cdw} , argue against a band-JT instability, even though electron-lattice coupling is ubiquitous to TMD [17].
- (iv) Finally, in spite of the incoherent metal features pointed out above, the effective mass is only weakly renormalised above T_{cdw} .

These observations put strong constraints on an acceptable theory. Most importantly, they conflict with both FS nesting and band-Jahn-Teller (JT) views on general grounds: Absence of band quasiparticles in the normal state rules out a conventional ordering instability involving the LDA Fermi surface (FS) features. Simply put, the very concept of a well-defined FS in the LDA sense becomes untenable in bad metals. As pointed out above, ARPES data also argue against a band-JT instability to CDW order. Weak mass renormalisation above T_{cdw} conflicts with one-band modeling, but not with a multi-band approach [18]: even in the classic Mott case of V_2O_3 , the effective mass in the correlated metal is only moderately enhanced near the (undoubtedly correlation driven) metal-insulator transition [18, 19]. Thus, taken together, these observations force one to view emergence of the CDW as a strong coupling Overhauser instability of a multi-band bad-metal normal state without LFL quasiparticles.

These issues have been selectively addressed earlier within conflicting theoretical views, but the above observations force us to critically re-examine them. Here, we show that these anomalous responses are naturally understood within our PEL view [7] for 1T-TiSe₂, strongly supporting the PEL as a novel (and perhaps generic) alternative to conventional theories for TMD. In remarkable parallels with d and f -band systems close to Mottness and unconventional order(s), we unravel a new instance of a selective metallic state in the PEL, and construct a scenario for the instability of this PEL to a

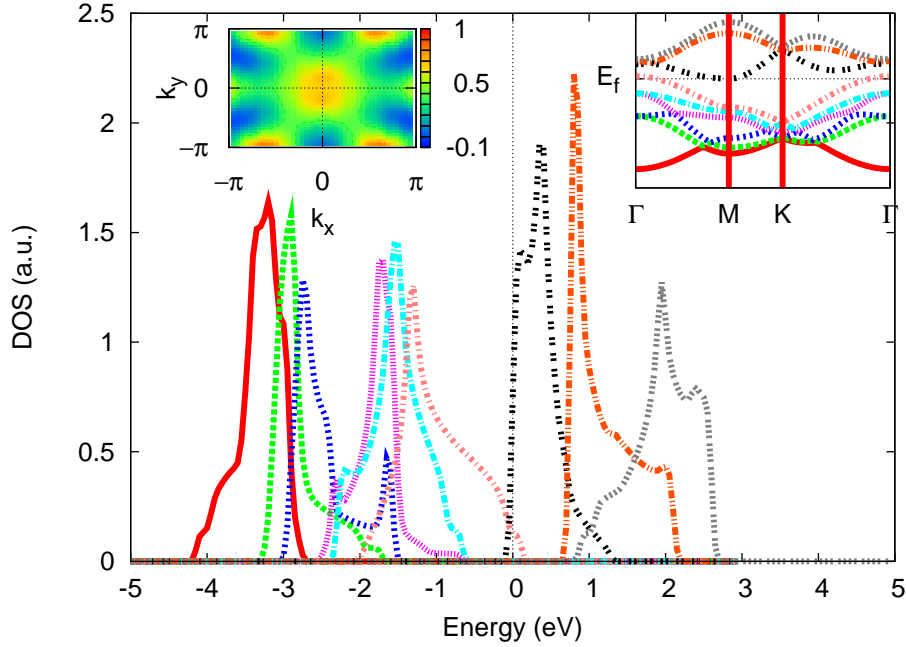


Figure 1. (Color Online) Non interacting DOS, tight binding band structure for the Ti-d t_{2g} and Se-p bands and the corresponding Fermi surface plot. The MO DMFT involves Ti-d (black) and Se-p (yellow) bands.

low- T CDW state. Our philosophy is opposite in spirit to weak-coupling Fermi liquid ones, and is actually closer to resonating valence bond (RVB) ideas [20], in the sense that ordered state(s) arise as two-particle (BEC) instabilities of an incoherent liquid of preformed excitons.

2. Method

LCAO band structure for 1T-TiSe₂ was constructed [9, 21] by using the Ti- d and Se- p states. This gives two bands closest to E_F (predominantly Ti- d_{xy} and Se- p_z) as well as the FS in very good accord with earlier results [21], as shown in Fig. 1. A sizable $d_{xy} - p_z$ mixing hybridises the small number of electrons and holes. In this situation, even moderate electronic correlations (< 1.0 eV) facilitate exciton formation already at high T , as already discussed by Halperin *et al.* [5] in the sixties. Given that electronically active states comprise d_{xy} and p_z band states, an intraband Hubbard $U \simeq 1.0$ eV and interband correlation $U_{ab} \simeq 0.5 - 0.7$ eV are realistic values: these can be estimated from a first-principles, constrained-LDA calculation, and we believe [22] that these fall in the range quoted above.

Though static Hartree-Fock (HF) theory can now give a CDW *ground* state [16, 9], description of observed normal state incoherence, and in general, preformed liquid-like electronic states, lies outside its scope. Thus, the character and ordering instabilities of such bad metals *cannot*, by construction, be rationalised by appealing to static-mean-field theory: this can only be reliably accessed by approaches which can adequately

capture dynamical correlations. For 1T-TiSe₂, a minimal two-band Hubbard model as defined below is mandated by LCAO results, and adequate treatment of dynamical correlations underlying incoherent behavior is achieved by dynamical-mean field theory (DMFT). DMFT and cluster-DMFT approaches have, by now, a proven record of successfully treating strong dynamical fluctuations in correlated electronic systems, making them preferred tools of choice in the present context. The two-band Hubbard model we use is (calling $d_{xy} = a$ and $p_z = b$)

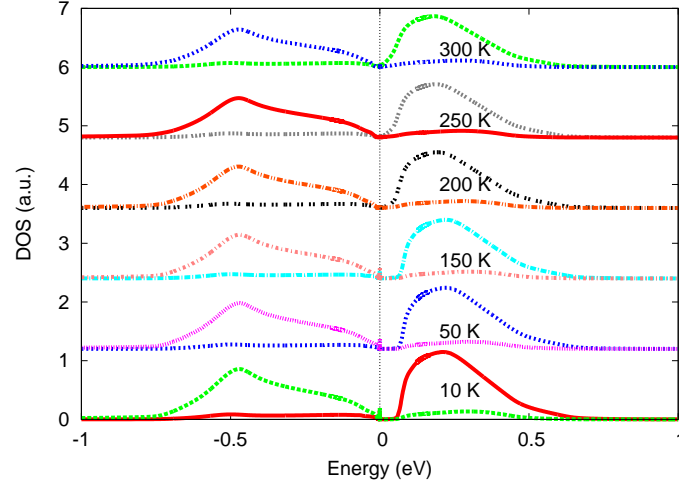
$$H_{el} = \sum_{\mathbf{k}, l, m, \sigma} (t_{\mathbf{k}}^{lm} + \epsilon_l \delta_{lm}) c_{\mathbf{k}l\sigma}^\dagger c_{\mathbf{k}m\sigma} + U \sum_{i, l=a, b} n_{il\uparrow} n_{il\downarrow} + U_{ab} \sum_i n_{ia} n_{ib}$$

where l, m run over both band indices a, b , the intra-orbital correlation is U (taken to be same for a, b bands, we have checked that results are insensitive to this choice within reasonable limits), U_{ab} is the inter-orbital correlation term that, along with $t_{\mathbf{k}}^{ab}$, will play a major role throughout. Further, in TMD, the most relevant A_{1g} phonon mode couples to the inter-band excitons [9] by symmetry, and the electron-phonon coupling is $H_{el-l} = g \sum_i (A_i + A_i^\dagger) (c_{ia}^\dagger c_{ib} + h.c.)$. To solve $H = H_{el} + H_{el-l}$ within DMFT, we have combined the multi-orbital iterated perturbation theory (MOIPT) for H_{el} [19] with the DMFT for polarons by Ciuchi *et al.* [23, 24] (see Appendix). Actually, this involves extending the polaron-DMFT to multiband cases, seen by writing $H_{el-l} = g \sum_i (A_i + A_i^\dagger) (n_{i,+} - n_{i,-})$ by a rotation, $c_{i,\pm} = (c_{i,a} \pm c_{i,b})/\sqrt{2}$ and $n_{i,\pm} = c_{i,\pm}^\dagger c_{i,\pm}$. Finally, as a theoretical advance, we extend the normal state DMFT to the broken-symmetry CDW phase as before [7]. This is justified, since, from the above discussion and LCAO+DMFT results below, we find, *a posteriori*, an incoherent PEL. Instability to CDW order then cannot occur via the traditional band-folding of well-defined Fermi liquid (FL) quasiparticles. Rather, as coherent one-particle inter-band mixing is inoperative, ordered states must now arise directly as two-particle instabilities of the bad metal. For 1T-TiSe₂, the residual two-particle interaction, obtained to second order is proportional to t_{ab}^2 , more relevant than the (incoherent) one-electron mixing, t_{ab} . The interaction $H_{res} \simeq -t_{ab}^2 \chi_{ab}(0, 0) \sum_{\langle i, j \rangle, \sigma\sigma'} c_{ia\sigma}^\dagger c_{jb\sigma'}^\dagger c_{jb\sigma} c_{ia\sigma}$, with χ_{ab} the inter-orbital susceptibility. Decoupling this intersite interaction in a generalised HF sense yields two competing instabilities: $H_{res}^{(HF)} = - \sum_{\langle i, j \rangle, \sigma\sigma'} (\Delta_{1b} c_{ia\sigma}^\dagger c_{ia\sigma} + \Delta_{ab} c_{ia\sigma}^\dagger c_{jb-\sigma}^\dagger + a \rightarrow b)$, with $\Delta_{cdw} = (\Delta_{1a} - \Delta_{1b}) \propto \langle n_a - n_b \rangle$ representing a CDW and $\Delta_{ab} \propto \langle c_{ia\sigma} c_{jb-\sigma} \rangle$ a multiband spin-singlet SC. Following earlier procedure [7], we compute DMFT spectral functions and transport properties in the CDW state at low T , leaving SC for future.

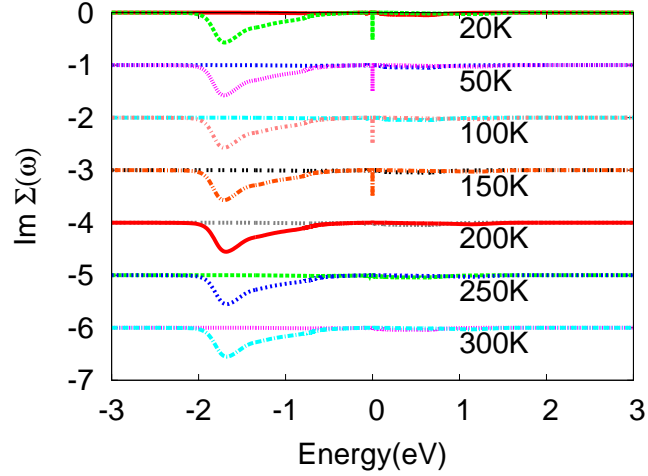
3. Results

We now show how the approach envisaged above gives a very good account of a whole range of physical responses. We show the DMFT many-body DOS for the ‘a’ (Ti-d) and ‘b’ (Se-p) bands in Fig. 2a and the corresponding self energies in Fig. 2b, 2c bands at high ($T > T_{cdw}$) and low ($T < T_{cdw}$) temperatures.

(a)



(b)



(c)

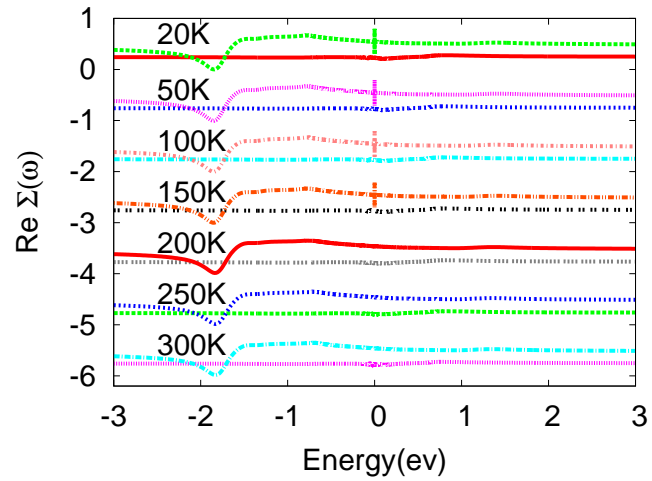


Figure 2. (Color Online) DMFT temperature evolution for (a) DOS of Ti-d and Se-p band (ones with peak below FL are for Se-p), (b) Imaginary part of self energy and (c) real part of self energy for Ti-d band and Se-p band. The self energies with a dip like structure close to -2 eV are for Se-p band.

The DOS shows clear ‘semi-metal’ features, which, however, are not those of a conventional semi-metal. Examination of the self-energies bares the hidden selective Mottness in the system: $\text{Im}\Sigma_a(\omega, T = 200 \text{ K})$ clearly shows incoherent metal features ($\text{Im}\Sigma_a(\omega = 0) > 0$ at $E_F(= 0)$), in accord with $(d\rho/dT) < 0$ for high- T (black dashed curve in Fig.2b), while the b -band continues to show renormalised band insulator-like features at low energy. This orbital-selectivity (OS) is thus related to strong normal state scattering, rather than the onset of CDW order. Finding of OS in 1T-TiSe₂ is surprising (Ti being nominally d^0), but can be traced back to the fact that, in presence of a small number of electrons and holes induced by t_{ab} , even a moderate U_{ab} leads to exciton formation, and thence to selective-Mottness in the multi-band situation that obtains in 1T-TiSe₂. Recall that the original idea of Mott was in fact indelibly tied to quantum melting of correlation-induced excitons under pressure. Intriguingly, in 1T-TiSe₂, stabilisation of excitonic CDW order enhances selective-Mott features at lower T , as emergence of the $\omega = 0$ pole in $\text{Im}\Sigma_{a,b}(\omega)$ clearly shows. Simultaneously, however, examination of $\text{Re}\Sigma_{a,b}(\omega)$ also clearly shows small mass enhancements. In extant literature [8], this finding below T_{cdw} is proposed as a concrete example of a *reduced* effective mass due to renormalisation effects caused by the appearance of a strong periodic potential below T_{cdw} . Our results are certainly in accord with this finding. As mentioned before, however, no large mass enhancements are theoretically (at least within DMFT) expected in a multiband system, even in an orbital-selective Mott regime. This goes hand-in-hand with slight stabilisation of the normal state gap, now interpreted as a true CDW gap. As advertised before, and in full accord with data, sizable T -driven SWT accompanies the transition.

If the PEL alternative is to be credible, the full range of observations must be explicable without any additional assumptions. In Fig. 3 we compare our DMFT one-particle spectral function, $A_{a,b}(\mathbf{k}, \omega) = -\text{Im}G_{a,b}(\mathbf{k}, \omega)/\pi$, and renormalised band dispersion, $E_{\mathbf{k},a,b} = \epsilon_{\mathbf{k},a,b} + \text{Re}\Sigma_{\mathbf{k},a,b}$, with ARPES data [16] where these exist. This is already a stringent test for theory: while LDA plus static-HF can conceivably yield agreement with band *dispersions*, the real test is a simultaneous description of the ARPES lineshapes. For a dynamically fluctuating ‘liquid’, the latter is expected to show broad continuum-like features without infra-red (LFL quasiparticle) poles. Rather remarkably, our LCAO+DMFT results provide an excellent semi-quantitative description of extant ARPES dispersions and lineshapes up to rather high energy. In particular, they bare the preformed excitonic features in $E_{\mathbf{k},a,b}$ and clear, associated ‘gap’ features in ARPES lineshapes above T_{cdw} . Excellent accord in all details, including the band positions, their intensity distributions, and band-shifts as a function of T , with the ARPES dispersion is clear from a direct comparison between our Fig. 4(a-c) with Fig.2 of Monney *et al.* [16] In particular, we can even identify the detailed features in the T -dependence of the ARPES intensity (Fig. 3) with data: (i) the peak at $\simeq -0.2 \text{ eV}$ is identified as the valence band backfolded to the M point by comparing the red curve in Fig. 3 with the top panel in Fig. 4. (ii) a new peak, labelled ‘C’ by Monney *et al.*, also appears below T_{cdw} and gets more pronounced upon decreasing T , precisely as

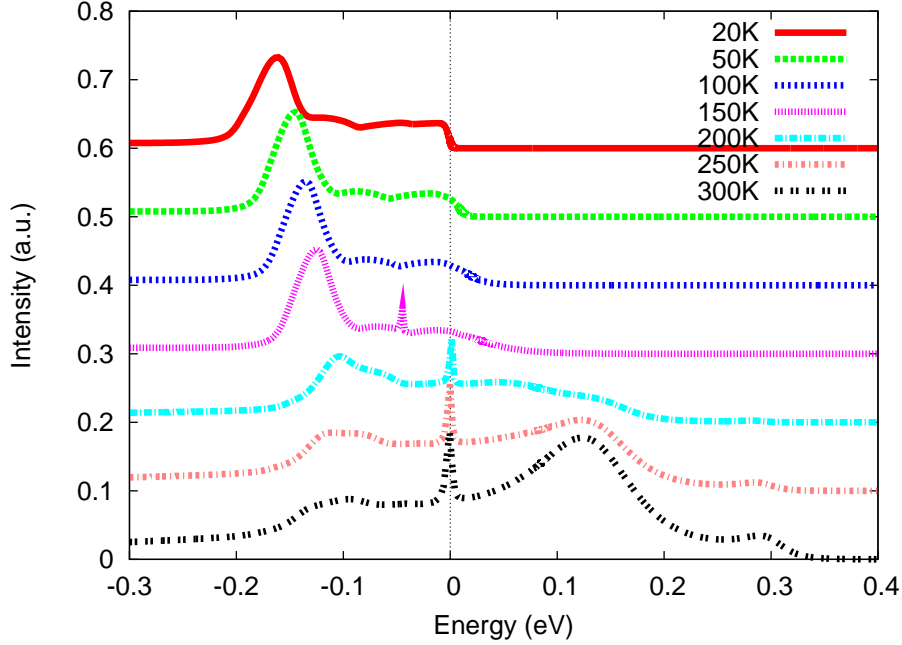


Figure 3. (Color Online) Theoretical ARPES at M point at different temperatures (T). As T increases across T_{cdw} , the peak in the DMFT spectral function crosses the renormalised Fermi energy (E_F).

seen. (iii) The peak ‘ D ’, identified as a ‘quasiparticle peak’ originating from coupling to phonons in experiment is also obtained in DMFT in very good qualitative accord with data: especially interesting is that it is quickly damped out as T increases, exactly as seen in the top four curves in our Fig. 3. However, at high T , we resolve an additional (sharper) low-energy peak, also arising from electron-phonon coupling, which remains dispersionless above T_{cdw} : this feature is not seen in the ARPES results of Monney *et al.* Finally, we also cannot observe peak ‘ A ’, identified with a second, spin-orbit split, valence band, since we have not used the full set of Se- p and Ti- d bands in this work. Nevertheless, the accord between theory and experiment is excellent with regard to features relevant for the CDW in 1T-TiSe₂.

We now consider the ARPES ‘band structure’ maps. At high- T , along K-M-K direction in the Brillouin zone the putative valence band, (VB) heavily damped by strong (due to preformed excitons) scattering, crosses $E_F (= 0)$ while the putative conduction band (CB) lies totally above E_F . This conflicts with the LDA (or LCAO, see Fig. 1) results, which predict a sizable overlap between VB and CB states at E_F , and reflects the failure of the FS nesting mechanism in the *real* one-particle spectra (in fact, to cure such conflicts, the standard explanation within conventional views has been to attribute such discrepancies between LDA and ARPES data to uncontrolled excess [8] of Ti. Our view naturally produces this, without having to take recourse to such extraneous conditions). Clear Hubbard-band shake-up features in DMFT are also seen in the color-plot: in particular, we predict that the $\omega > 0$ part of the lineshape (at M point in Fig. 4d) should lend itself to observation in inverse ARPES (ARIPES) studies in future. In addition,

Preformed Excitons, Orbital Selectivity, and Charge-Density-Wave Order in 1T-TiSe₂

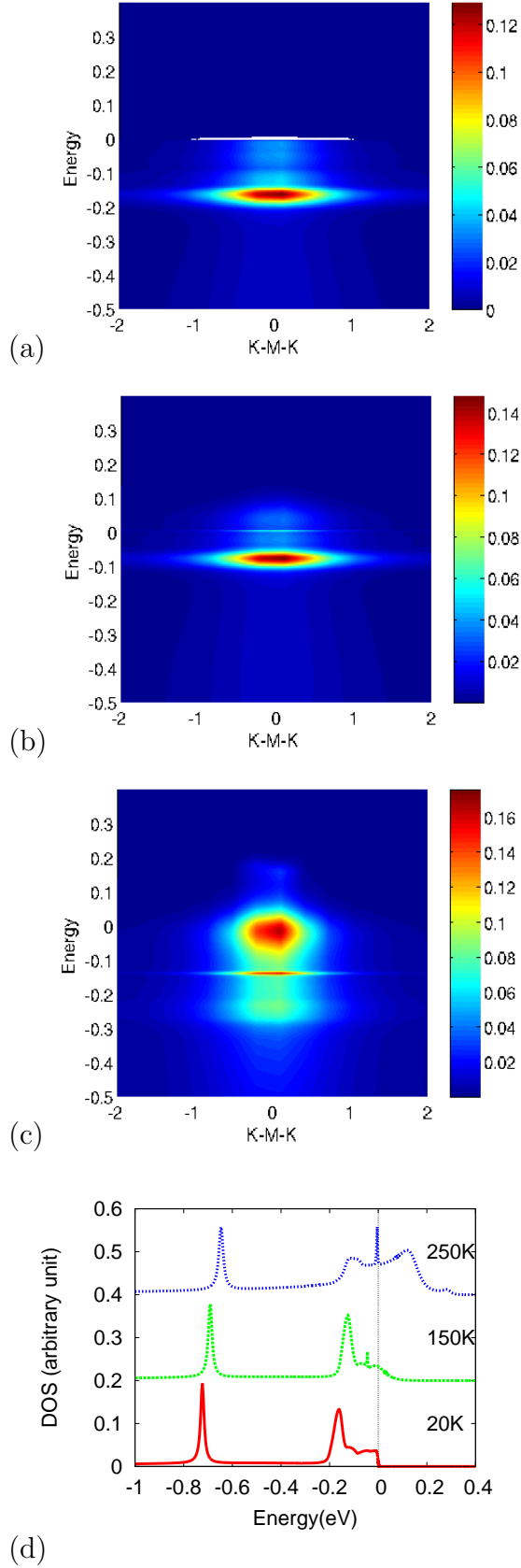


Figure 4. (Color Online) Theoretical ARPES map along K-M-K direction at (a) 20K (b) 150K (c) 270K (d) Total EDC at M point at different temperatures. Excellent accord with ARPES data is clearly seen.

comparison of the DMFT energy distribution curve (EDC) with extant ARPES result at the M point also shows (Fig.3) very good accord as a function of T over the whole range. A moderate band narrowing of LCAO bands and broad spectral lineshapes with appreciable T -dependent SWT in one single system are generic fingerprints of strong dynamical correlations in multi-orbital systems, and so, as alluded to before, the second feature above, essential for describing ‘liquid’ correlations, cannot be accounted for by a static-HF theory, as done so far [9].

Detailed Fermi surface (FS) maps as a function of T in 1T-TiSe₂ are rare. We have taken the FS mapped out by Rossnagel *et al.* [25] to study how the PEL idea survives this important test. While instabilities driven by LDA FS forms the backbone of weak coupling or itinerant views, it is also possible, in a renormalised itinerant or Mottness based theories, that these could involve a *new* FS sizably reconstructed by correlations. That the FS does not reconstruct across T_{cdw} in 1T-TiSe₂ was one of the main (among others, see above) arguments for invoking unconventional PEL scenarios in the first place. Close inspection of FS evolution across T_{cdw} shows that, while this is undoubtedly correct, there are still specific features which any theory needs to confront: (i) the band pockets are smeared out at high temperature ($T > T_{cdw}$) and, more importantly, a much brighter ring structure appears at the M point below T_{cdw} .

In Fig. 5, we show our DMFT FS at low (top panel) and high- T (bottom panel). As expected due to strong PEL scattering, the high- T FS is sizably smeared out (arises from the finite $\text{Im}\Sigma_a(\omega = 0)$ at 200K from Fig. 2). Remarkably enough, we *also* find a clear ring feature at the M point below 150K (lower panels), in remarkable accord with data. Since this ring-like feature becomes well-defined only below T_{cdw} , it is a direct consequence of CDW order-induced reconstruction of electronic states. This is fully consistent with the excitonic CDW view, where CDW follows excitonic ‘solid’ order, and the latter arises principally via interplay between $t_{ab}^{\mathbf{k}}$ and U_{ab} , implying backfolding of Se p band from the Γ point due to the 2x2x2 CDW superstructure formation. Further, close observation of DMFT results shows that the central pocket around the Γ point has seemingly developed ‘elongated’ shape instead of the hexagonal shape expected from the LCAO result. We believe that this important modification, hitherto not noted sufficiently, arises due to an orbital-dependent electronic structure reconstruction that is essentially driven by the \mathbf{k} -dependent form factor of the inter-orbital hybridisation ($t_{ab}(\mathbf{k})$). Experimental confirmation of this feature would thus constitute additional support for a PEL scenario. Finally, the stabilisation and slight increase of the normal state ‘gap’ below T_{cdw} also accords with optical data [13] and with the semi-metal-to-semiconductor characterisation of the normal-CDW transition in 1T-TiSe₂.

Thus, such quantitative agreement between our excitonic-DMFT results premised upon a novel PEL view and ARPES in all important details lends strong credence to the idea of a dynamically fluctuating excitonic liquid at high T giving way to a low- T CDW order. However, to further qualify as a credible candidate, the *same* formulation must also describe transport as well. Fortunately, in DMFT, this task is simplified: it is an excellent approximation to compute transport co-efficients directly from the DMFT

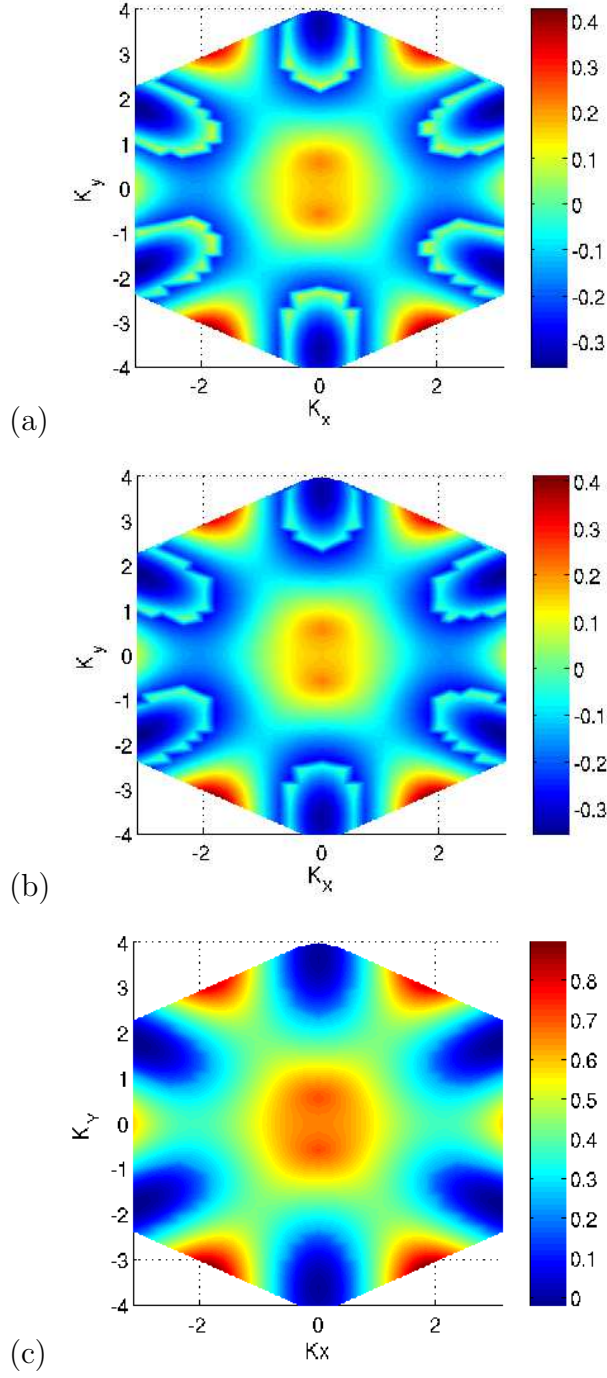


Figure 5. (Color Online) DMFT FS map at (i) 20K (ii) 150K (iii) 270K, showing very good agreement with the T-evolution of the Fermi surface in ARPES data of Rossnagel *et al.* [25]

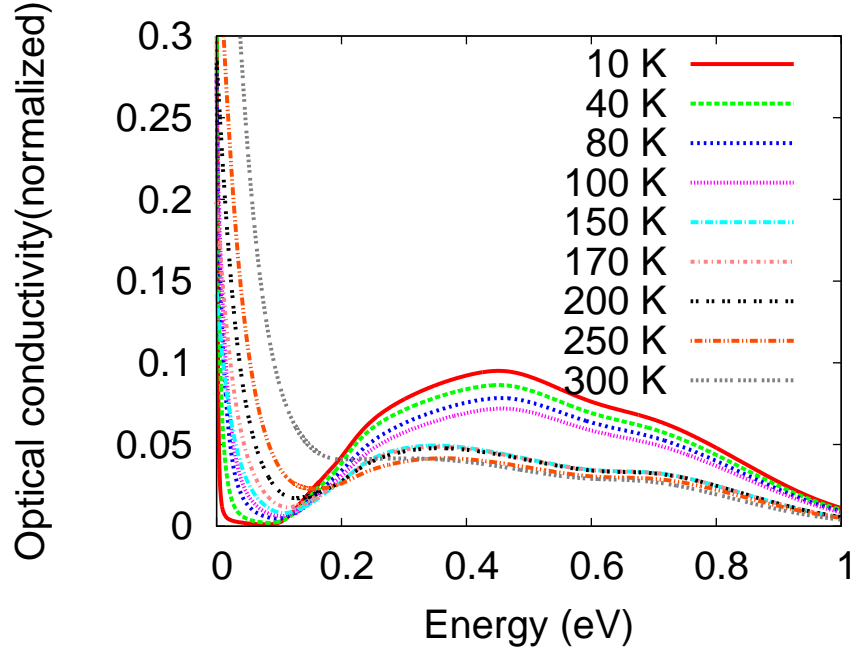


Figure 6. (Color Online) DMFT results for T -dependent optical conductivity, showing good agreement with optical data across T_{cdw} .

propagators $G_{a,b}(k, \omega)$ [26], since (irreducible) vertex corrections rigorously vanish for one-band models, and turn out to be surprisingly small even for the multi-band case.

In Fig. 6, we show the optical conductivity $\sigma(\omega)$ as a function of T , wherein very good accord with data up to an energy $\simeq O(0.8)$ eV is clear. A clean CDW gap at low T closes rapidly with increasing T via rapid spectral weight transfer from the relatively sharply defined hump at 0.4 eV to the infra-red regions, precisely as seen. Given that we have kept only the two bands crossing E_F in LCAO, agreement at higher energy (≥ 0.8 eV) is not expected. The relative sharpness of the low-energy optical response at low T is deceptive: it is not a FL Drude peak, and in fact, (fully consistent with the selective-Mott behavior in the DMFT spectra above) no FL coherence sets in, even at lowest (10 K) T in DMFT. It is rather a reflection of reduced incoherence due to CDW gap opening. Finally, we also resolve an isosbestic point in $\sigma(\omega, T)$ curves (where $\sigma(0.2\text{eV})$ remains invariant) at different T : this is clear manifestation of sizable dynamical correlations [7], and is again in good accord with the isosbestic point seen around 0.27 eV in the optical study [13].

The DMFT resistivity (Fig. 7) also shows an insulator-like behavior above T_{cdw} , a broad peak without any anomaly below $T_{cdw} = 200$ K, and bad metallic behavior below T_{cdw} , in full accord with data [14]. The insulator-like behavior for $T > T_{cdw}$ is a reflecting of the large normal state incoherence, whence carriers strongly scatter off fluctuating, incoherent (preformed) excitons. The bad-metallic behavior below T_{cdw} is then naturally attributable to reduction of this strong normal state scattering due to (i) opening up of a CDW gap, and (ii) concomitant increase in the tendency to excitonic coherence. Given the bad-metallic resistivity, the consequent short scattering mean-

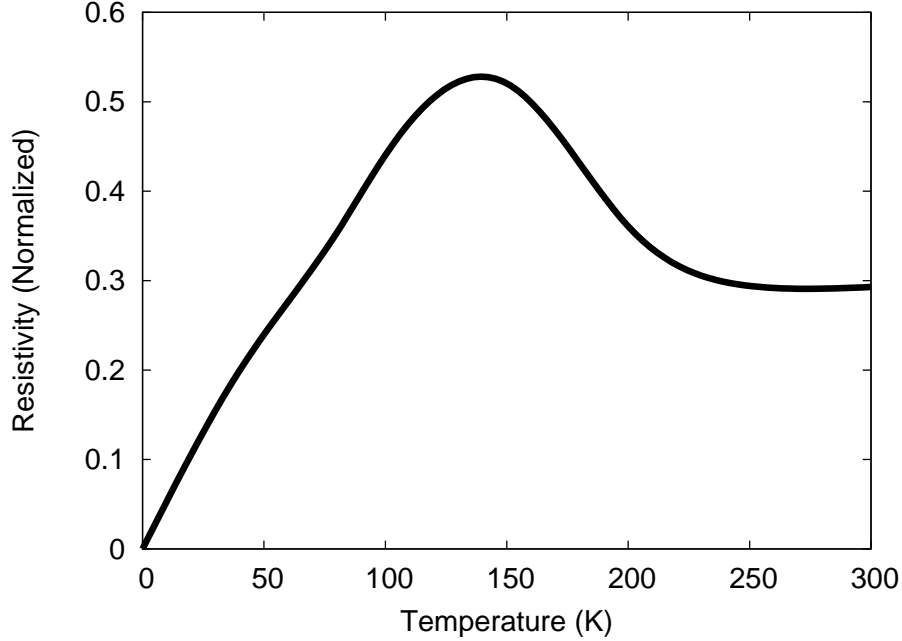


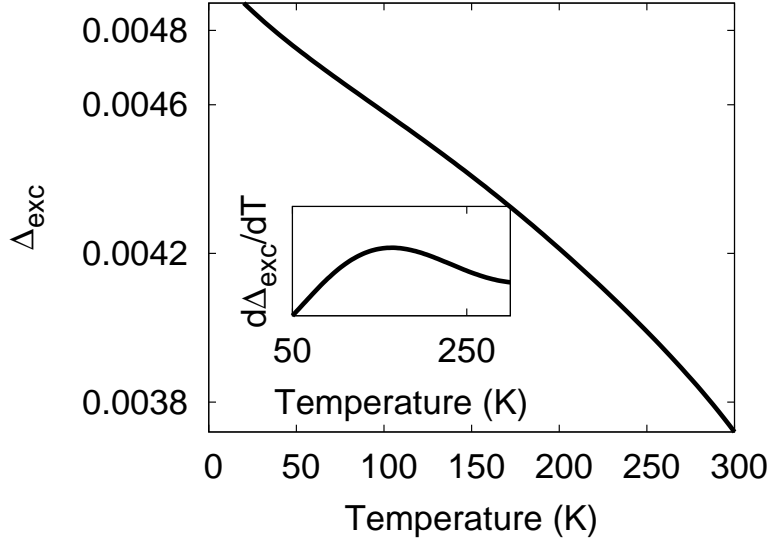
Figure 7. T -dependent dc resistivity within DMFT. Except for the low- T part, LCAO+DMFT results agree very well with experimental results, including a broad maximum, rather than any sharp non-analytic change, across T_{cdw} (see text).

free path (in fact, $k_F l \simeq O(1)$) invalidates a quasiclassical Boltzmann equation-based approach to transport. Interestingly, this is precisely the regime where DMFT should work best. The absence of a sharp ordering anomaly at T_{cdw} is additional evidence against a weak coupling view of the instability. In fact, in a weak-coupling instability, resistivity should have shown a sharp ordering anomaly at T_{cdw} on general grounds [27] (in addition, $d\rho/dT$ must also show critical behavior, with exponents linked to those extracted from thermodynamic measurements). The strong coupling view is further supported by finding of a large $2\Delta/k_B T_{cdw} \simeq 7 - 10$ in TMD (about 7 for 1T-TiSe₂ and 10 for 2H-TaSe₂ [28]). This feature is reminiscent of high- T_c cuprates [29] and implies that CDW formation is associated with a BEC, rather than a BCS-like scenario for the exciton instability. Also, strong inelastic scattering needed to rationalise bad-metallicity above T_{cdw} and sizable T -induced SWT are characteristic signatures of a strong coupling limit.

Thus, taken together, very good accord with ARPES and transport data strongly supports our basic hypothesis: (i) the normal state is a strongly fluctuating liquid of incoherent excitons, and (ii) CDW order in 1T-TiSe₂ must fall into the strong coupling class, qualitatively different from a conventional Overhauser transition of well-defined band (LFL) quasiparticles.

Emergence of CDW order from a PEL should leave further specific signatures in other data. First, CDW and excitonic correlations must now track each other beyond T_{cdw} , well into the PEL state. In Fig. 8, we show the excitonic and CDW order parameters, $\Delta_{exc} \propto \langle \Gamma^x \rangle = \langle (c_{ia}^\dagger c_{ib} + h.c.) \rangle$, $\Delta_{cdw} \propto \langle \Gamma^z \rangle = \langle n_a - n_b \rangle / 2$, along with their

(a)



(b)

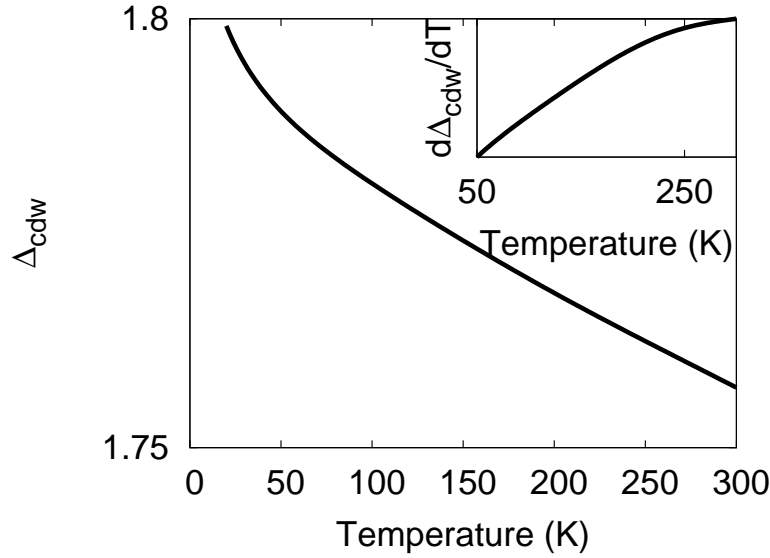


Figure 8. (a) Expectation values and derivative (inset) of inter-orbital excitonic ($\text{Im}G_{ab}$), and of (b) CDW order parameter, $n_a - n_b = \Delta_{cdw}$ and its derivative (inset) as a function of T .

T -derivatives, as a function of temperature (T). In particular, as expected in the PEL scenario, *both* follow each other and are finite way above T_{cdw} , in nice qualitative accord with the T -dependence of the CDW order parameter from ARPES [16]. The absence of a conventional (BCS-like) mean-field transition can be rationalised by noticing that, in presence of the el-lattice coupling, $H_{el-l} = g \sum_i (A_i + A_i^\dagger)(c_{ia}^\dagger c_{ib} + h.c.)$, the universality class of the normal-CDW transition turns out to be that of an Ising model in an external field. This implies that the (mean-field) transition is smeared into a smooth crossover. The relevance of excitonic correlations is also visible as follows. We see that $\rho(T)$ closely follows the T -dependence of $d\Delta_{exc}/dT$ above (Fig. 8), but does not show any

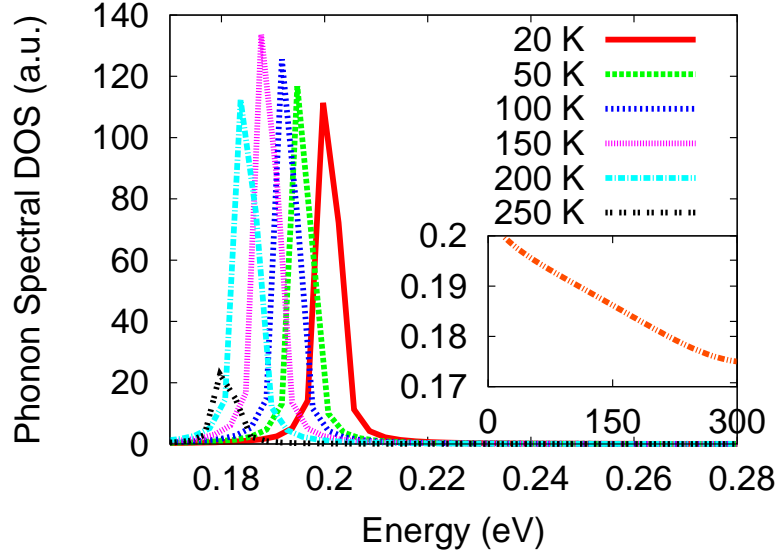


Figure 9. (Color Online) Phonon spectral function at different temperatures. The inset shows change in peak position of the A_{1g} phonon mode with T , in good accord with Raman data above T_{cdw} (see text).

obvious correlation with $d\Delta_{cdw}/dT$: this shows that the anomalous resistivity is caused by carriers scattering off incoherent excitonic (liquid-like) correlations. In our PEL scenario, the change to metallic behavior in $\rho(T)$ is attributable to reduction of the strong scattering when excitons condense at T_{cdw} . True CDW order now follows a true BEC of preformed excitons at lower T .

Given the specific form of the electron-phonon coupling, now also interpretable as coupling of interband excitons to A_{1g} phonon mode by symmetry, the lattice is expected, very generally, to react to the T -dependent changes (incoherent at high T , more coherent at lower T) in exciton dynamics. In particular, the DMFT phonon spectral function, computed from $\rho_{ph}(\omega) = (-1/\pi)\text{Im}D(\omega) = (-1/\pi)\text{Im}[2\Omega_0/(\omega^2 - \Omega_0^2 - 2g^2\Omega_0\chi_{ab}(\omega))]$ and shown in inset of Fig. 9, should mirror excitonic CDW correlations.

Several interesting features stand out: (i) $\rho_{ph}(\omega)$ shows maximum intensity with reduced linewidth around $T_m = 150$ K, precisely where the resistivity peaks. (ii) Above T_{cdw} , the phonon spectrum is noticeably broader, reflecting coupling to incoherent excitonic liquid modes, and (iii) asymmetry in $\rho_{ph}(\omega)$ *increases* as T is lowered below T_{cdw} . This reflects precursors of a Fano-like structure, arising from treatment of H_{el-l} beyond the adiabatic limit within our DMFT. Onset of excitonic coherence below T_{cdw} reduces strong normal state scattering, sharpening the phonon spectrum. (iv) Finally, we find that the detailed T -dependence of both the A_{1g} -phonon lineshape and linewidth excellently matches that extracted from a Raman scattering study [30]. Only below T_{cdw} is there a discord between measured and computed linewidths: it levels off to a constant in experiment, a feature not captured by our present calculation. The reason is that we have not carried out a study of the change in phonon dynamics below T_{cdw} . A full study of lattice effects must rest on a more realistic input to the full phonon

spectrum of 1T-TiSe₂, a point we leave for future study. Thus, taken together, very good quantitative accord with a whole host of spectral and transport responses for 1T-TiSe₂ and a comprehensive qualitative rationalisation of structural features in one single theoretical picture constitutes overwhelming support for a novel PEL view. Thus, the central conclusion of our work is: *The CDW instability must now be interpreted as a strong coupling instability of an incoherent PEL normal state, rather than as a weak coupling Fermi surface nesting instability of a good LFL.*

The above findings have important implications for SC arising under pressure. A finite pressure increases $a - b$ band overlap via t_{ab} , leading to a redistribution of electrons and holes, and weakens excitonic CDW order. From Fig. 8a, this implies enhancement of excitonic fluctuations, also seen by noticing that a fall of $\langle \Gamma_i^z \Gamma_j^z \rangle$ must transfer weight to the transverse part, i.e, enhance $\langle (\Gamma_i^+ \Gamma_j^- + h.c) \rangle$ via the pseudospin sum-rule $\mathbf{\Gamma}^2 = \Gamma(\Gamma + 1)$. Thus, near the critical $p = p_c$ where CDW is destroyed, we expect a maximisation of excitonic fluctuations. These can constitute the critical collective (electronic) fluctuations that could lead to an instability to an inter-band SC (competing with CDW) with a finite $\Delta_{ab} \simeq \langle c_{ia\sigma} c_{jb-\sigma} \rangle$. However, normal state incoherence implies that SC must now arise directly from the incoherent metal via a two-particle instability: this can be explored by solving $H = H_{el} + H_{res}$ in the pair channel. The el-lattice coupling will further enhance the effective pair interaction in H_{res} above [7]. Even without the benefit of a detailed DMFT calculation for the SC phase, we thus expect the SC T_c to be maximal close to p_c if dynamical excitonic fluctuations mediate cooper pairing: this is again in accord with observations [14] and the causal link is compelling.

We believe the present work also has further important implications on a broader level. Our unexpected finding of OS bad-metallicity in the high- T PEL brings 1T-TiSe₂ closer to the bad actors in d - and f -band systems, where OS is a consequence of orbital-selective Hubbard correlations [31] (or, in the cuprates, momentum-selective correlations [29]). Given that 1T-TaS₂ has long been known to be a Mott insulator, our proposal of selective-Motttness and associated excitonic liquid features is quite reasonable, albeit novel. However, since magnetism is never an issue in the TMDs of interest, what underpins anomalous responses reminiscen of d - and f -band critical systems near magnetism is moot. The common unifying mechanism seems to be selective-Motttness, which is indeed one of the main contenders for understanding anomalous quantum criticality in d and f -band systems [32, 33]. Selective-Motttness itself can always occur via different mechanisms: in particular, depending upon the microscopics of a given system, it can be associated with magnetism, but it clearly does not always need to be so. It can also be associated with other density-wave instabilities in the charge or orbital sectors in mutliband systems such as TMDs. Nevertheless, a common element, namely destruction of Landau FL quasiparticles, would always accompany onset of selective-Motttness. Thus, in light of the present work, it should not be too surprising that the high- T PEL bears some similarities with the FL* theory [32] in the f -electron QCP context. Evidence attesting to this comes from the fact that

only the Se- p band crosses E_F , while the Ti- d band lies above E_F already in the high T liquid. In other words, the observed FS has already reconstructed from its LDA counterpart to reflect the preformed excitonic character of the normal state. Spectral and transport features show characteristic incoherence features, as expected in an FL* state, and the efficacy of DMFT as a valuable tool to understand these is also known in the f -electron context [34, 31]. That this identification implies an interesting scenario, similar to those invoked for anomalous metals on the border of ($T = 0$) magnetism may also permit a rationalisation of the apparent ‘similarities’ claimed to exist between under-doped cuprates and TMD [10]. Viewed from the perspective of our study, these similarities are, ultimately, manifestations of the selective-(bad) metallicity in both cases: momentum-selective in under-doped cuprates, and orbital-selective in 1T-TiSe₂. Thus, we arrive at a perhaps general idea with broader appeal across classes of correlated systems: Selective Mottness (whether orbital or momentum) induces critical electronic liquid states characterised by loss of LFL coherence. This collectively fluctuating electronic fluid can subsequently become unstable, either to a myriad (charge, spin, orbital) of density wave orders, or to (competing) unconventional superconductive orders, depending upon the actual microscopics of the system under study. In TMD, material specific reasons favor competing inter-band CDW and SC orders from such a strongly fluctuating excitonic liquid.

4. Conclusion

In conclusion, we show that a whole host of physical responses in 1T-TiSe₂, difficult to reconcile with a band FS nesting or band-JT mechanisms, is provided a natural and good quantitative explication within a new PEL alternative. Finding of novel, orbital-selective Mott features in renormalised normal state electronic structure via DMFT leads to an excellent description of a range of spectral and transport data in both normal and CDW states. More importantly, it brings the TMD closer to the anomalous critical metals of much more recent interest. Along with its success for 2H-TaSe₂ [7], our work relates the PEL idea to a more generic theoretical level for TMD. Particularly interesting should be to test how this new proposal fares for the even more correlated 1T-TaS₂ [35], which is undoubtedly a known Mott insulator [12], as well as competition between CDW and SC, in future work.

SK acknowledges CSIR (India) for a senior research fellowship. MSL thanks the ILL Grenoble for financial support and hospitality. We thank H Cercellier for very helpful discussions.

5. Appendix

5.1. Tight binding band structure

TiSe₂ is a layered material with hexagonal layers of Ti sandwiched between layers of Se atoms: a 1T-polytype transition metal dichalcogenide. The Ti d-band is in a d^0 state in TiSe₂. Due to octahedral coordination the Ti atom d-shell is split into a set of high energy e_g orbitals and low lying, degenerate t_{2g} orbitals. We consider only the low lying t_{2g} orbitals, for, they are the ones that form the hybridized bands with Se-p orbitals close to the Fermi level. In the LCAO calculation, therefore, we consider charge transfer between them and the surrounding Se 4p orbitals, so that six Se p orbitals and three Ti d orbitals per unit cell are involved. Our results are similar to those of Wezel *et al.* [9], but we do not invoke quasi-1D features resulting from the orbital dependence of the hopping matrix elements as the driving cause of CDW. However, the shape of the central pocket around the Γ point in the DMFT Fermi surface in the main text does hint toward such anisotropic features getting more pronounced in the CDW ordered phase.

The tight binding Hamiltonian is thus constructed as

$$\begin{aligned}
 \hat{H} = & \sum_{i,\alpha} \frac{\Delta}{2} (\hat{d}_{i,\alpha}^\dagger \hat{d}_{i,\alpha} - \hat{p}_{1i,\alpha}^\dagger \hat{p}_{1i,\alpha} - \hat{p}_{2i,\alpha}^\dagger \hat{p}_{2i,\alpha}) \\
 & + \sum_{\langle i,j \rangle, \alpha, \beta} (t_{\alpha,\beta,i-j}^{dd} \hat{d}_{i,\alpha}^\dagger \hat{d}_{j,\beta} + t_{\alpha,\beta,i-j}^{pp} [\hat{p}_{1i,\alpha}^\dagger \hat{p}_{1j,\beta} - \hat{p}_{2i,\alpha}^\dagger \hat{p}_{2j,\beta}]) \\
 & + \sum_{\langle i,j \rangle, \alpha, \beta} (t_{\alpha,\beta,i-j}^{pd} [\hat{d}_{i,\alpha}^\dagger \hat{p}_{1j,\beta} + \hat{d}_{i,\alpha}^\dagger \hat{p}_{2j,\beta} + H.c.] + \\
 & t_{\alpha,\beta,i-j}^{pp} [\hat{p}_{1i,\alpha}^\dagger \hat{p}_{2j,\beta} + H.c.]). \tag{5.1.1}
 \end{aligned}$$

Here \hat{d}_i^\dagger , \hat{p}_{1i}^\dagger and \hat{p}_{2i}^\dagger create electrons on the Ti, the upper Se and the lower Se atom respectively. The labels α and β run over all possible orientations of the Ti $d_{t_{2g}}$ and Se p orbitals and $\langle i, j \rangle$ denotes neighbouring sites. t^{dd} , t^{pp} and t^{pd} are the different hopping matrices for d and p orbitals and Δ is the chemical potential.

This Hamiltonian results in a 9×9 matrix using Slater-Koster integrals, and several matrix elements vanish rigorously due to crystal symmetry. We obtain the LCAO band structure by diagonalizing the resultant matrix. By adjusting the values of Slater-Koster integrals and the chemical potential the tight binding bands can be fit to the extant LDA calculation. Setting $dd\sigma = -0.2$, $dd\pi = 0.2$, $dd\delta = -0.5$, $pd\pi = 0.5$, $pp\sigma = 0.4$ and $\Delta = 2.0$ we get a TB fit in good quantitative agreement with the LDA results [21, 36].

5.2. Electron phonon Self Energy

To calculate electron-phonon self-energy we incorporate the procedure first used by Ciuchi et al. [23] (using Einstein phonons) into our multi-orbital DMFT. The local intra- and inter-orbital Coulomb correlations are treated upto second order selfconsistent multiband IPT as usual. Since both Hubbard and electron-phonon interaction terms are local, their combined effect can be treated simultaneously within DMFT. Contribution of the electron-phonon coupling to electronic self energy is given by

$$g^2 \sum_{i\omega_n} G_0(p) D_0(\omega) = g^2 \left[\frac{N_q + n_f(\zeta_p)}{ip_n + \omega_q - \zeta_p} + \frac{N_q + 1 - n_f(\zeta_p)}{ip_n - \omega_q - \zeta_p} \right] \quad (5.2.1)$$

Where $N_q = \frac{1}{e^{\beta\omega_q} - 1}$.

The full Hamiltonian, including excitonic coupling of phonons is

$$\begin{aligned} H = & \sum_{k,a,b,\sigma} (t_k^{ab} + \epsilon_a \delta_{ab}) c_{ka\sigma}^\dagger c_{kb\sigma} + U \sum_{i,\mu=a,b} n_{i\mu\sigma} n_{i\mu-\sigma} + U_{ab} \sum_i n_{ia} n_{ib} + g \sum_i (c_{a\sigma}^\dagger c_{b\sigma} + h.c.) (A_i^\dagger + A_i) \\ & - V \sum_i c_{b\sigma}^\dagger c_{b\sigma} (1 - c_{a\sigma}^\dagger c_{a\sigma}) + \omega_0 \sum_i A_i^\dagger A_i. \end{aligned} \quad (5.2.2)$$

We start with an initial ansatz for the self energy $\Sigma_{int}(\omega) = Un + A\Sigma_0^{(2)}(\omega)$ where $\Sigma_0^{(2)}(\omega)$ is the second order contribution of electron-electron and interband excitons coupling to A_{1g} phonons. The IPT scheme is that we calculate lattice Green's function (G_{fa}) from this full self energy, from which the bare Green's function is found via the Dyson equation: $G_{0a}^{-1} = G_{fa}^{-1} + \Sigma_a$. Plugging this G_{0a} back into the IPT, we obtain a new estimate of $\Sigma_{0a}^{(2)}$ and this procedure is iterated to convergence.

Having both Hubbard-like and el-ph couplings changes the estimate of A_{ab} used in the interpolative self-energy in IPT as follows. Following usual procedure, A_{ab} is calculated from the condition that it reproduce the leading behavior of the (of the exact atomic limit) self-energy at high frequency. The leading behavior for large ω can be obtained by expanding the Green function in a continuous fraction [37]: $G_{fa}(k, \omega) = 1/(\omega - \epsilon_{fa} - M_{1a} - \frac{M_{2a} - M_{1a}^2}{\omega + \dots})$. Here, M_i denotes the i th order moment of the density of states. One can compute these quantities by evaluating a commutator[38], and for the model above, $M_{2a} - M_{1a}^2 = U_{ab}^2 (n_{fa}(1 - 2n_{fa}) + \langle n_{fa} n_{fb} \rangle) + g^2 (n_{fa+} + n_{fa-})$. Here, n_{fa} is the number density calculated from the full Green's Function, $n_{fa+} = g^2 \sum_\omega (G_f(\omega + \omega_q)(N_q + n_f(\omega)))$ and $n_{fa-} = g^2 \sum_\omega (G_f(\omega - \omega_q)(N_q + n_f(-\omega)))$. From the large frequency limit of (1), $\Sigma_{0a}^2(\omega) = U_{ab}^2 n_{0a}(1 - n_{0a}) + g^2 (n_{0a-} + n_{0a+})$. Here, n_{0a} is a fictitious number density of the 'bare' Green's function. Explicitly, $n_{0a+} = g^2 \sum_\omega (G_0(\omega + \omega_q)(N_q + n_f(\omega)))$ and $n_{0a-} = g^2 \sum_\omega (G_0(\omega - \omega_q)(N_q + n_f(-\omega)))$. Comparing with the exact high-frequency limit, we thus have $A_{ab} = \frac{U_{ab}^2 (n_{fa}(1 - 2n_{fa}) + \langle n_{fa} n_{fb} \rangle) + g^2 (n_{fa+} + n_{fa-})}{U_{ab}^2 n_{0a}(1 - n_{0a}) + g^2 (n_{0a-} + n_{0a+})}$.

Within the DMFT approximation, the phonon self-energy turns out to be $\Pi(q, \omega) = \frac{g^2 \chi_c(q, \omega)}{1 + g^2 \chi_c(q, \omega) D_0(q, \omega)}$ where $\chi_c(q, \omega)$ is the usual charge-charge response function [39] and

$D_0(q, \omega)$ is the bare phonon Green's function. $\chi_c(q, \omega)$ is estimated by a renormalised bubble contribution of the DMFT Green functions. We ignore the irreducible vertex corrections, since their contribution should be small for the small number of electrons and holes that characterise the two-band system close to an excitonic insulator/liquid regime, and is a further approximation.

6. References

- [1] M. Imada et al; Revs. Mod. Phys, **70**, 1039 (1998)
- [2] Y. Kamihara et al; J. Am. Chem. Soc., **128**, 10012 (2006)
- [3] M. Imada, et al., J. Phys.: Condens. Matter **22**, 164206 (2010).
- [4] J A Wilson, et al., Adv. Phys. **24**, 117 (1975).
- [5] B. I. Halperin, et al., Rev. Mod. Phys. **40**, 755 (1968).
- [6] H Cercellier, et al., Phys. Rev. Lett. **99**, 146403 (2007).
- [7] A Taraphder et al., Phys. Rev. Lett. **106**, 236405 (2011).
- [8] C. Monney *et al.*, Europhys. Lett. **92**, 47003 (2010); C. Monney, et al., Phys. Rev. Lett **109**, 047401 (2012).
- [9] J van Wezel, et al., Europhys Lett. **89**, 47004 (2010).
- [10] F. Weber, et al; Phys. Rev. Lett. **107**, 266401 (2011); S. V. Borisenko et al., Phys. Rev. Lett. **100**, 196402 (2008).
- [11] Dordevich, et al; Euro. Phys. Jour. B. , (20)
- [12] P. Fazekas, E. Tosatti, Philos. Mag. B **39**, 229 (1979).
- [13] G. Li, et al., Phys. Rev. Lett. **99**, 027404 (2007).
- [14] A. Kuzmartseva, et al., Phys. Rev. Lett. **103**, 236401 (2009).
- [15] B. Lake, et al., Science **291**, 1759 (2001).
- [16] C. Monney, et al., Phys. Rev. B **81** 155104 (2010).
- [17] K. Held et al; Phys. Rev. Lett. **86**, 5345 (2001).
- [18] M. S. Laad et al; Phys. Rev. Lett. **91**, 156402 (2003).
- [19] A. Poteryaev et al; Phys. Rev. B **76**, 085127 (2007).
- [20] P W Anderson, Science **235**, 1196 (1987).
- [21] Y. Yoshida and K. Motizuki, J. Phys. Soc. Jpn. **49**, 898 (1980).
- [22] A Yaresko, private communication.
- [23] S. Ciuchi, et al., Europhys. Lett **24** 575 (1993).
- [24] S. Koley , N. Mohanta and A. Taraphder, AIP Conf. Proc. **1461**, 170 (2012).
- [25] K. Rossnagel, et al., Phys. Rev. B **65**, 235101 (2002).
- [26] J. Tomczak and S. Biermann, *Phys. Rev. B* **80**, 085117 (2009).
- [27] M. Fisher and J. Langer, PRL **20**, 665 (1968)
- [28] W. L. McMillan, Phys. Rev. **167**, 331 (1968)
- [29] M. Civelli et al., Phys. Rev. Lett. **100**, 046402 (2008)
- [30] C. S. Snow, et al., Phys. Rev. Lett. **91**, 136402 (2003).
- [31] M. S Laad, S. Koley and A. Taraphder, *J. Phys.: Condens. Matter* **24**, 232201 (2012).
- [32] P. Ghaemi *et al.*, *Phys. Rev. B* **75**, 144412 (2007); *ibid Phys. Rev. B* **77**, 245108 (2008).
- [33] S. Sachdev, *Phys. Rev. Lett.* **105**, 151602 (2010).
- [34] A Georges, et al., Rev. Mod. Phys. **68**, 13 (1996).
- [35] B Sipos, et al. Nat. Mater. **7**, 960 (2008).
- [36] R. A. Jishi, et al., Phys. Rev. B **78** 144516 (2008).
- [37] R. G. Gordon, J. Math. Phys. (N.Y.) **9**, 655 (1968).
- [38] W. Nolting and W. Borgie, Phys. Rev. B **39**, 6962 (1989).
- [39] O Gunnarsson, et al., J. Phys. Condens. Matter **20**, 043201 (2008)